Angewandte Chemie
Eine Zeitschrift der Gesellschaft Deutscher Chemiker

Supporting Information

An Efficient Labelling Approach to Harness Backbone and Side-Chain Protons in ^{1}H-Detected Solid-State NMR Spectroscopy

Deni Mance, Tessa Sinnige, Mohammed Kaplan, Siddarth Narasimhan, Mark Daniëls, Klaartje Houben, Marc Baldus, and Markus Weingarth**

anie_201509170_sm_miscellaneous_information.pdf

Table of contents:

S1 QUANTITATIVE ANALYSIS OF THE ^{1}H PATTERN IN FD UBIQUITIN

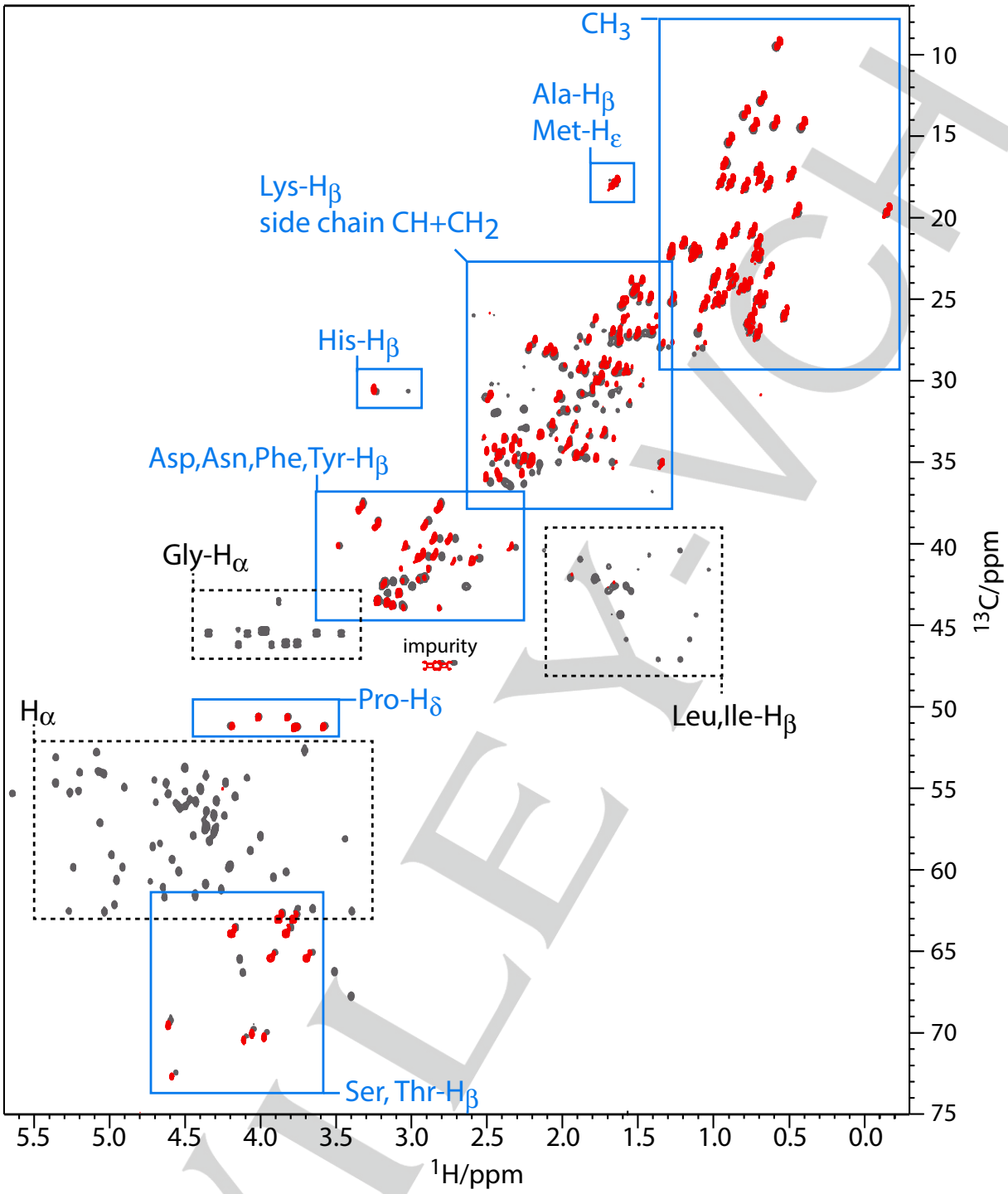

Figure S1. Superposition of solution-state NMR ^{13}C-^{1}H HSQC[1] spectra measured with fully protonated (FP, in grey) and fractionally deuterated (FD, in red) ubiquitin. Spectra were measured at 900 MHz ^{1}H frequency. Spectral regions in which FD ubiquitin showed only very weak signals (such as the Hα region) due to very low protonation level are highlighted in dashed black boxes. Spectral regions in which FD ubiquitin showed intense signals are highlighted in blue boxes. See below (Table S1 and Figure S2) for further analysis of the ^{1}H pattern. ^{1}H, ^{13}C and ^{15}N solution NMR assignments were taken from Ref. ([2]).

	Hα	Hβ	Hγ	Hγ2	Hδ	Hδ2	Hε
Ala	1	26					
Arg	1	7	38		31		
Asp	1	42					
Asn	1	41					
Cys	*						
Gln	1	8	29				
Glu	1	8	29				
Gly	1						
His	1	30					
Ile	1	3	18	40		37	
Lys	1	30	46		26		4
Met	8	*	56		*		
Pro	1	2	33		35		
Leu	1	5	0		40	40	
Phe	1	24					
Ser	1	90					
Thr	3	30	19				
Trp	*						
Tyr	1	21					
Val	1	0	40	44			

Table S1. ^{1}H-populations [%] in FD ubiquitin in comparison to FP ubiquitin. The ^{13}C-^{1}H HSQC spectra were normalized (to account for different sample concentrations) following the procedure outlined in Ref. ([3]) and referenced to ^{15}N-^{1}H HSQC spectra. All analysis was based on ^{1}H, ^{13}C and ^{15}N solution NMR assignments from Ref. ([2]). Subsequently, well-resolved signals (which was the majority of the signals) in the ^{13}C-^{1}H HSQC spectra were integrated in Topspin 3.2 (Bruker) and their intensities compared. Note that ubiquitin features no Cys nor Trp residues, which could hence not be analyzed. However, Cys residues share a common metabolic pathway with Ser residues and therefore presumably feature a high degree of protonation at Cβ. The Hβ population of Met could not be assessed due to spectral overlap. Hβ with populations above 20 % (in blue) could be readily assigned in 3D CCH experiments, while Hβ with populations below 8 % (in red) were either entirely absent or showed very weak signals.
Note that many methylene Cβ featured slightly unequal protonation levels for the two directly attached ^{1}H. This was most pronounced for His (Hβ1: 56 % protonation; Hβ2: 4 % protonation) and Lys (Hβ1: 40 % protonation; Hβ2: 19 % protonation) residues.

Detailed biochemical explanations for the observed ^{1}H levels in FD proteins can be found in Ref.([4]). Indeed, much of the ^{1}H pattern in FD ubiquitin can be deduced by means of the standard-textbook amino acid biosynthesis pathway:

- Hα protons are virtually absent because all amino acids recruit their Hα protons from the solvent during transamination of a precursor α-keto acid.
- the branched-chain amino acids (Val, Ile, Leu), which have the lowest ^{1}H levels at Cβ, are pyruvate-derived (their Cβ corresponds to the *deprotonated* C2-oxo group of pyruvate).
- amino-acids derived from a-ketoglutarate (Arg, Glu, Gln, Pro) also feature low ^{1}H levels at Cβ.
- Ser-Cβ features an exceptionally high ^{1}H level because it is derived from 3-phosphoglyerate and the Cβ corresponds to the $C6H_2$ of glucose.

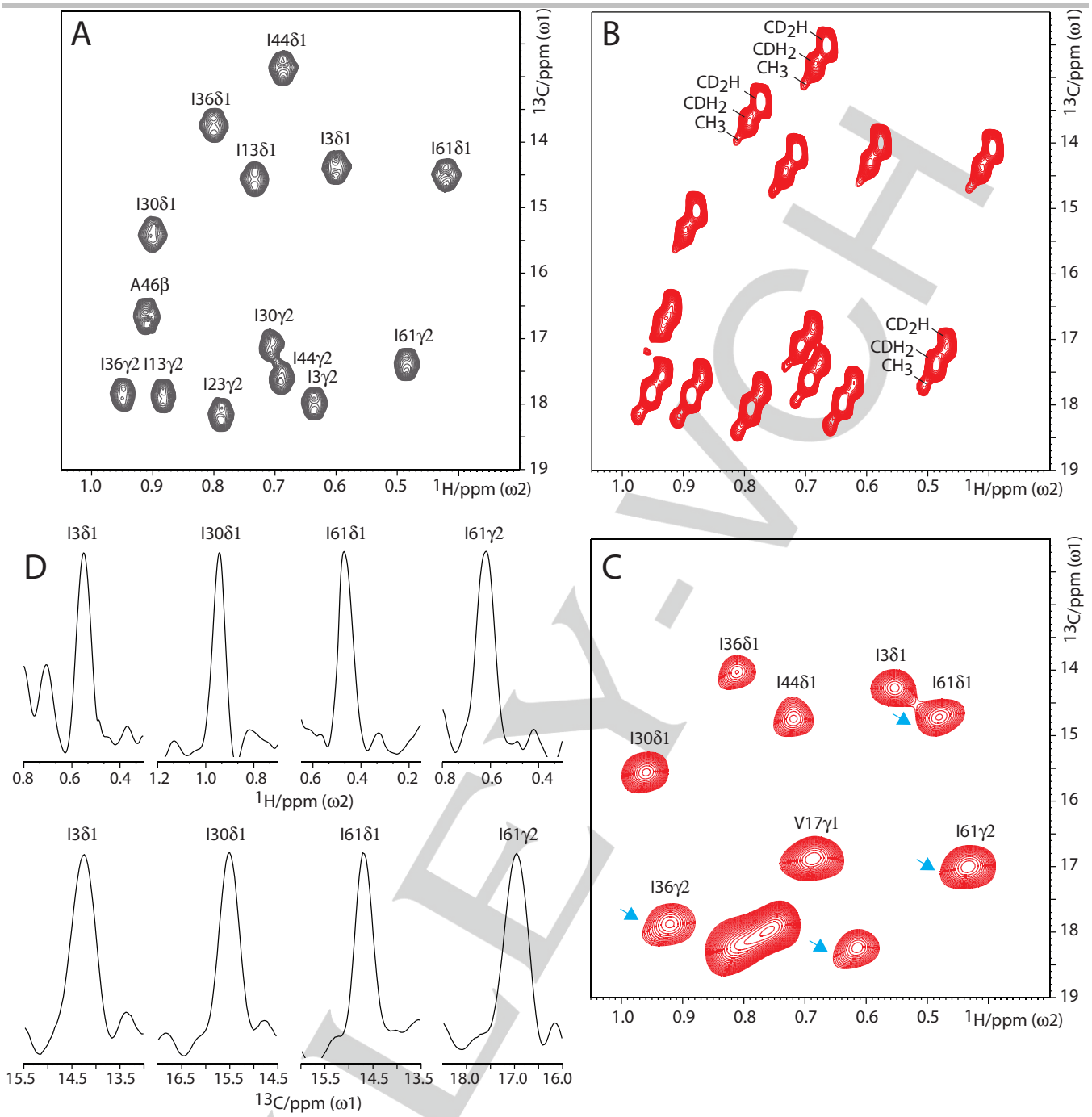

Figure S2. Comparison of methyl-signals in 2D CH HSQC spectra. A) Fully protonated ubiquitin; solution-state NMR. B) Fractionally deuterated ubiquitin; solution-state NMR. The methyl-signals show the typical splitting in CH_3, CDH_2 and CD_2H resonances. Note that the amino-acid specific populations of the different isotopomers in fractionally deuterated proteins have been analysed in detail by Otten et al.[3]. C) Fractionally deuterated ubiquitin; solid-state NMR. While some CH_3 signals featured a slightly oval shape (marked with blue arrows), we generally did not observe significant broadening due to isotopomer effects, presumably because fully protonated CH_3 or CH_2 carbons are much broadened in comparison to CDH and CD_2H/CDH_2 peaks, respectively. However, isotopomer effects may become more visible at higher spinning frequencies >100 kHz MAS,[5] where the fully protonated carbons presumably can be observed. D) 1D slices through the ^{13}C (top) and ^{1}H (bottom) dimensions of selected cross-peaks from the spectrum shown in C).

S2 EXPERIMENTAL SECTION

S2.1 Solid-state NMR

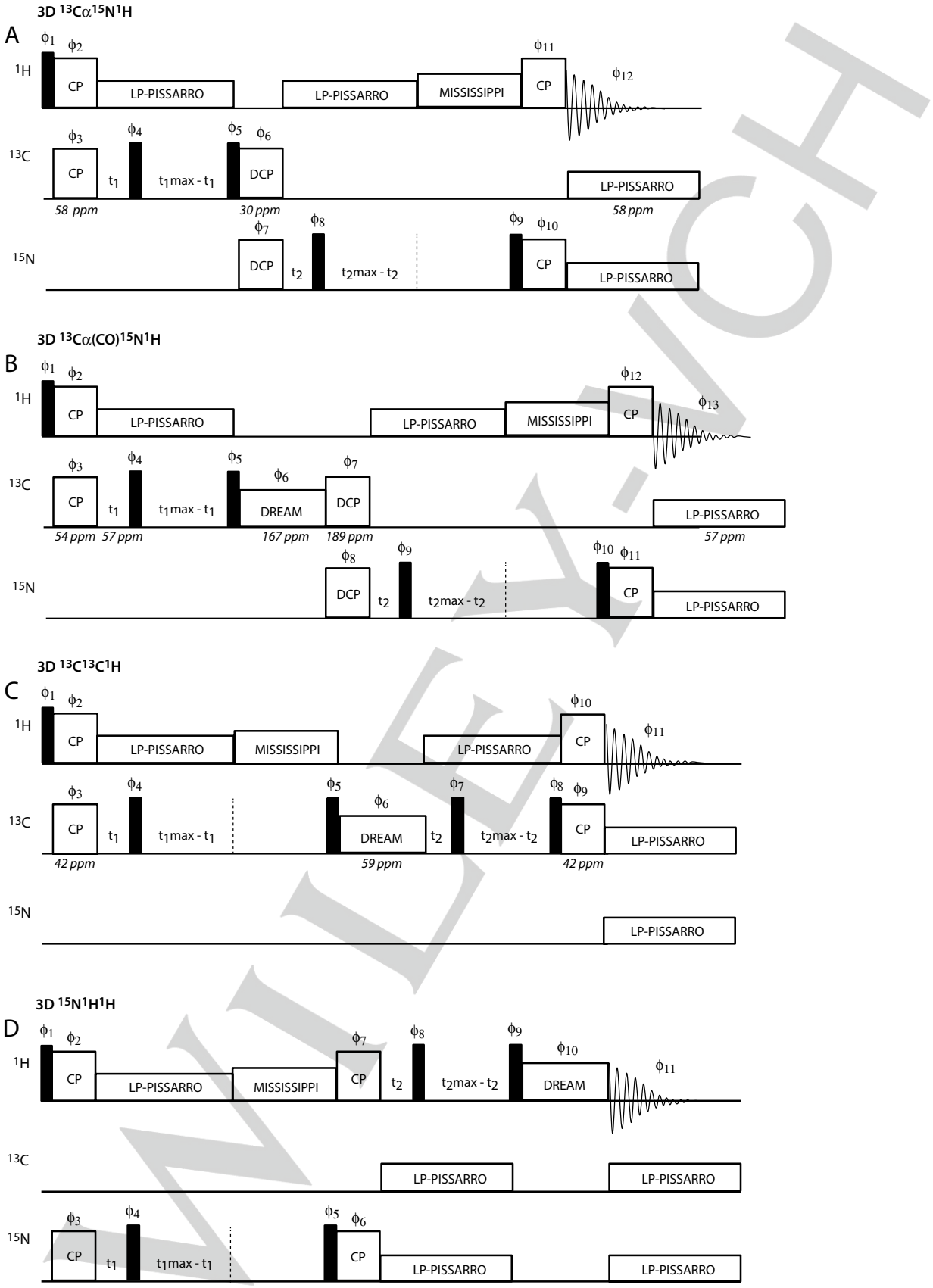

Figure S3. Illustration of the ^{1}H-detected 3D pulse sequences used in this study.

All experiments were carried out at 18.8 T static magnetic field (800 MHz ^{1}H frequency) and 52 kHz MAS if not indicated otherwise. The sample temperature was set to 300 K. Water suppression was achieved with the MISSISSIPPI[6] scheme. Decoupling was performed with the PISSARRO[7] scheme during all direct and indirect acquisition periods. For all experiments and all nuclei, the decoupling amplitude was set to one quarter of the MAS frequency, i.e., 13 kHz. Decoupling times were optimized and set to 31.5 µs for ^{1}H decoupling, 47.6 µs for ^{13}C decoupling and 53 µs for ^{15}N decoupling. For all experiments, quadrature-detection in the indirect dimensions was achieved using TPPI. The pulse sequence used to acquire 2D ^{13}C/^{15}N-^{1}H spectra was described in Ref. ([8]). For all 2D spectra / planes shown in the manuscript and the Supporting Information, we used a contour level increment of 1.05 – 1.10 and 50 – 60 contour levels.

A) 3D CαNH experiments. The initial ^{1}H -> ^{13}C transfer was brought about with ramped (20 %) cross polarization contact times of 3.5 ms and 2.4 ms for FD ubiquitin and FD KcsA, respectively. The chemical shifts were encoded in the indirect dimensions in a constant-time (CT) manner[9] (constant time means here (defined in Ref. ([9])) that the total duration of i) the duration of the indirect evolution time + ii) the duration of subsequent z-filter is constant) during low-power PISSARRO decoupling. Polarization was transferred further from ^{13}Cα -> ^{15}N with SPECIFIC CP[10] using 37 kHz irradiation on ^{13}C and 15 kHz irradiation on ^{15}N during 5.5 ms for both FD ubiquitin and FD KcsA. Despite the relatively strong irradiation on the ^{13}C channel, DCP transfer was specific for Cα, which was achieved by moving the ^{13}C carrier upfield (to 30 ppm), away from the CO signal region. No decoupling on ^{1}H was necessary during DCP transfer, since heteronuclear dipolar couplings involving ^{1}H are efficiently suppressed at 52 kHz MAS in fractionally deuterated proteins. The final transfer from ^{15}N -> ^{1}H was carried out with cross-polarization (36 kHz on ^{15}N, 90 kHz on ^{1}H, 400 µs contact time for FD ubiquitin, 500 µs for FD KcsA). The measurement time was 20h for ubiquitin and 5d 20h for KcsA.
Phase cycling: f_1: x ; f_2: y, -y ; f_3: y ; f_4: -x ; f_5: x ; f_6: y ; f_7: x ; f_8: -y, -y, -y, -y, y, y, y, y, y, y, y, y, -y, -y, -y, -y ; f_9: y, y, y, y, y, y, y, y, -y, -y, -y, -y, -y, -y, -y, -y ; f_{10}: x, x, -x, -x, -x, -x, x, x, x, x, -x, -x, -x, -x, x, x ; f_{11}: y ; f_{12}: x, -x, -x, x, x, -x, -x, x, x, -x, -x, x, x, -x, -x, x

B) 3D Cα(CO)NH experiments. The initial ^{1}H -> ^{13}C transfer was brought about with ramped (20 %) cross polarization contact times of 3.5 ms and 2.4 ms for FD ubiquitin and FD KcsA, respectively. The ^{13}C carrier was set to 54 ppm, which yielded selective transfer to aliphatic carbons (Figure S4). After CT-t_1 evolution, magnetization was transferred from ^{13}Cα -> ^{13}CO with the DREAM recoupling using 23 kHz recoupling amplitude over 6.5 ms (FD ubiquitin) / 5.5 ms (FD KcsA). The sweep through the HORROR condition was performed with a linear amplitude ramp (20 % ramp). Best transfer performance was achieved with the ^{13}C carrier close to the ^{13}CO region (167 ppm) during the transfer. No subsequent suppression of Cα polarization was applied, since the latter spectral region was virtually depleted of signal after DREAM[11] recoupling. No ^{1}H-decoupling was applied during DREAM recoupling, which did not lead to any perceivable transfer losses in comparison the application of ^{1}H-decoupling. The following ^{13}CO –> ^{15}N –> ^{1}H transfer steps were analogous to those described in the 3D C_aNH experiments. For the ^{13}CO –> ^{15}N DCP transfer, contact times of 6.5 ms (FD ubiquitin) and 5.5 ms (FD KcsA) were used. The measurement time was 3d 20h for ubiquitin and 9d 20h for KcsA. The time requirement for KcsA was reduced by applying non-uniform sampling (65 %). Reconstruction was performed with compressed sensing[12] in Topspin 3.2 (Bruker Biospin).
Phase cycling: f_1: y, -y ; f_2: x ; f_3: x ; f_4: -y ; f_5: y ; f_6: x ; f_7: x, x, -x, -x, -x, -x, x, x, x, x, -x, -x, -x, -x, x, x ; f_8: x ; f_9: -y, -y, -y, -y, y, y, y, y, y, y, y, y, -y, -y, -y, -y ; f_{10}: y, y, y, y, y, y, y, y, -y, -y, -y, -y, -y, -y, -y, -y ; f_{11}: x ; f_{12}: x ; f_{13}: x, -x, -x, x, x, -x, -x, x, x, -x, -x, x, x, -x, -x, x

C) 3D CCH experiment. After ^{1}H -> ^{13}C cross-polarization transfer (3.5 ms contact time) and CT-t_1 evolution, ^{13}C - ^{13}C mixing was brought about with double quantum DREAM recoupling using 27 kHz recoupling amplitude (20 % ramp) over 3.0 ms. The transfer time was relatively short to select for one-bond ^{13}C – ^{13}C transfer and the ^{13}C carrier during the transfer set to 59 ppm. No ^{1}H decoupling was applied during the recoupling time. After CT-t_2, polarization was transferred from ^{13}C –> ^{1}H in a CP step, which was kept relatively short (275 us) to select for one bond ^{13}C – ^{1}H transfer. The measurement time was 4d 22h for ubiquitin.
Phase cycling: f_1: y, -y ; f_2: x ; f_3: x ; f_4: -y, -y, -y, -y, y, y, y, y, y, y, y, y, -y, -y, -y, -y ; f_5: y, y, y, y, y, y, y, y, -y, -y, -y, -y, -y, -y, -y, -y ; f_6: x ; f_7: -y ; f_8: y ; f_9: x, x, -x, -x, -x, -x, x, x, x, x, -x, -x, -x, -x, x, x ; f_{10}: y ; f_{11}: x, -x, -x, x, x, -x, -x, x, x, -x, -x, x, x, -x, -x, x

D) 3D NHH experiment. After ^{1}H -> ^{15}N cross-polarization transfer (1.8 ms contact time) and CT-t_1 evolution as well as subsequent water-suppression, polarization was transferred back to ^{1}H (400 µs contact time). ^{1}H – ^{1}H polarization transfer was brought about with dipolar DREAM double quantum recoupling over 3.0 ms using a recoupling amplitude of 27 kHz. The measurement time was 5d 7h for ubiquitin and 4d 22h for KcsA. The time requirement for KcsA was reduced by applying non-uniform sampling (65 %). For KcsA, we used a shorter ^{1}H-^{1}H mixing time (750 us) and 58 kHz MAS. Note that we also acquired 2D N(H)H experiments for open-inactivated KcsA with 750 µs and 1.5 ms DREAM ^{1}H-^{1}H mixing.

Phase cycling: f_1: x ; f_2: y, -y ; f_3: x ; f_3: f_4: -y, -y, -y, -y, y, y, y, y, y, y, y, -y, -y, -y, -y ; f_5: y, y, y, y, y, y, y, y, -y, -y, -y, -y, -y, -y, -y, -y ; f_6: x, x, -x, -x, -x, -x, x, x, x, x, -x, -x, -x, -x, x, x ; f_7: y ; f_8: x ; f_9: -x ; f_{10}: y ; f_{11}: x, -x, -x, x, x, -x, -x, x, x, -x, -x, x, x, -x, -x, x

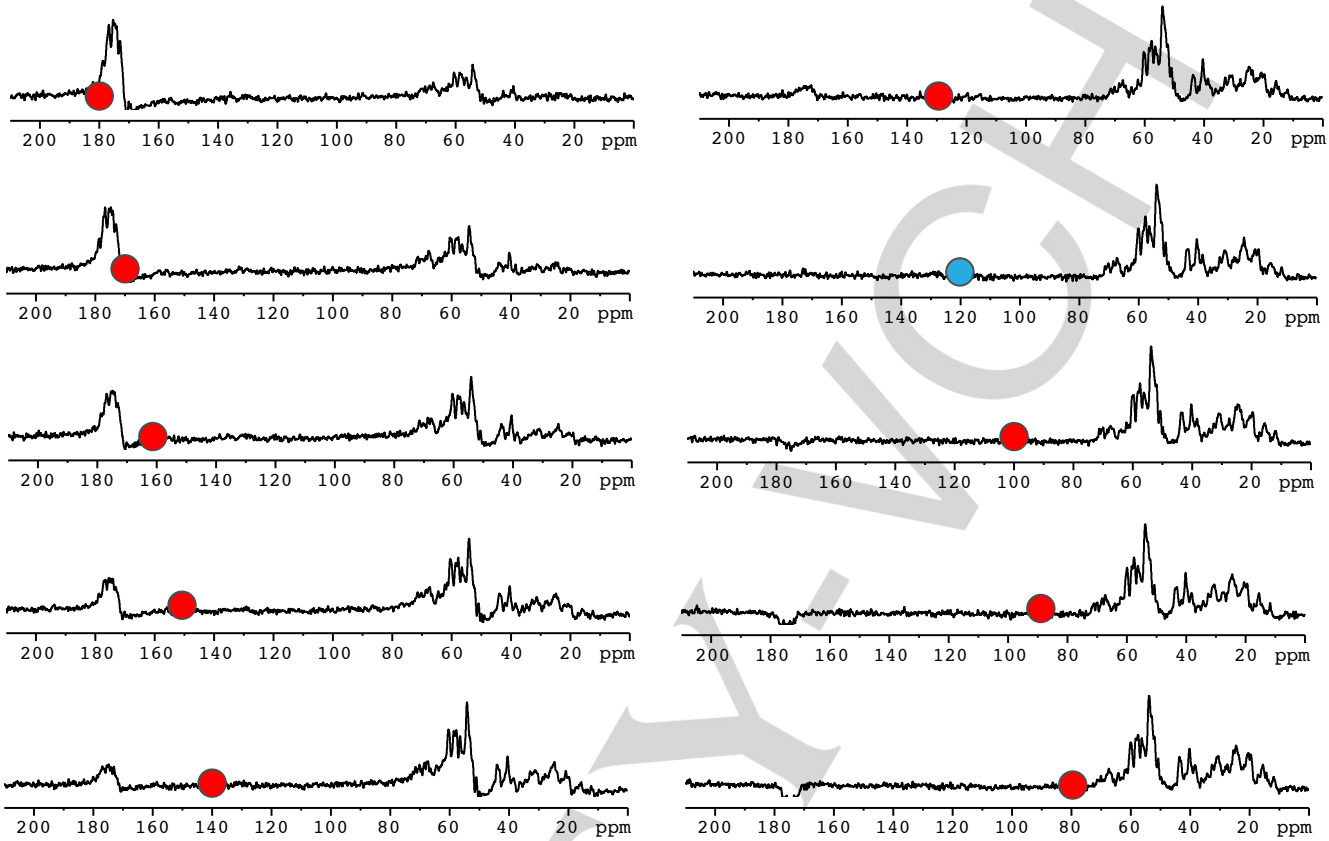

Figure S4. Selective ^{1}H -> ^{13}C cross-polarization. By sweeping the ^{13}C carrier from low to high field, a condition (here around 120 ppm, blue dot) could be obtained at which the CP transfer is selective for aliphatic carbons. The optimal ^{13}C carrier position depends on the CP condition. This 'selective' CP can be used as a preparatory step for the 3D C_a(CO)NH experiment, which saves one transfer step in comparison to a preparatory ^{15}N -> ^{13}Cα transfer element.

S2.2 SOLUTION NMR

Liquid-state ^{1}H-detected ^{13}C-^{1}H and ^{15}N-^{1}H HSQC[1] spectra of FD and FP [^{15}N,^{13}C] labeled ubiquitin were recorded at 298 K on at 900 MHz ^{1}H frequency and equipped with a cryogenic TXI probe. To avoid bias due to differences in relaxation, a long recycle delay of 2s was used for both samples.

S2.3 NMR SIMULATIONS

All simulations were carried out with the SPINEVOLUTION[13] software (version 3.5.0). Simulations were performed to demonstrate that the cross-polarization (CP) transfer from Cα to H^N is much enhanced in the absence of Hα protons, which correlates with the strong $C\alpha H^N$ cross peaks in ^{13}C – ^{1}H spectra of fractional deuterated proteins (see Figures 1A main text and S8). The NMR theoretical reason for the enhanced transfer is that the transfer across the weak $C\alpha H^N$ dipolar coupling is not truncated by strong CαHα dipolar couplings in fractional deuterated proteins.[14]

^{13}C – ^{1}H ramped CP simulations were carried out with the 3-spin system H^N–Cα–Hα with the typical geometry of a peptide plane. To probe the effect of the strong CαHα dipolar coupling on the transfer across the weak C_aH^N coupling, the CαHα distance was successively increased from 1.08 Å to 2.48 Å in steps of 0.1 Å while the C_aH^N

distance was keep constant at 2.15 Å. Dipolar H^N – Hα couplings were switched off during the entire simulated experiment.

The magnetization was initially on the ^{13}C nucleus and finally detected on the H^N nucleus. Simulations were performed at 50 kHz MAS and 800 MHz magnetic field, close to the experimental conditions. CSA contributions had no significant effect on the simulations and were omitted in the following.

S3 ASSIGNMENTS IN FD UBIQUITIN AND FD KCSA

S3.1 FD UBIQUITIN

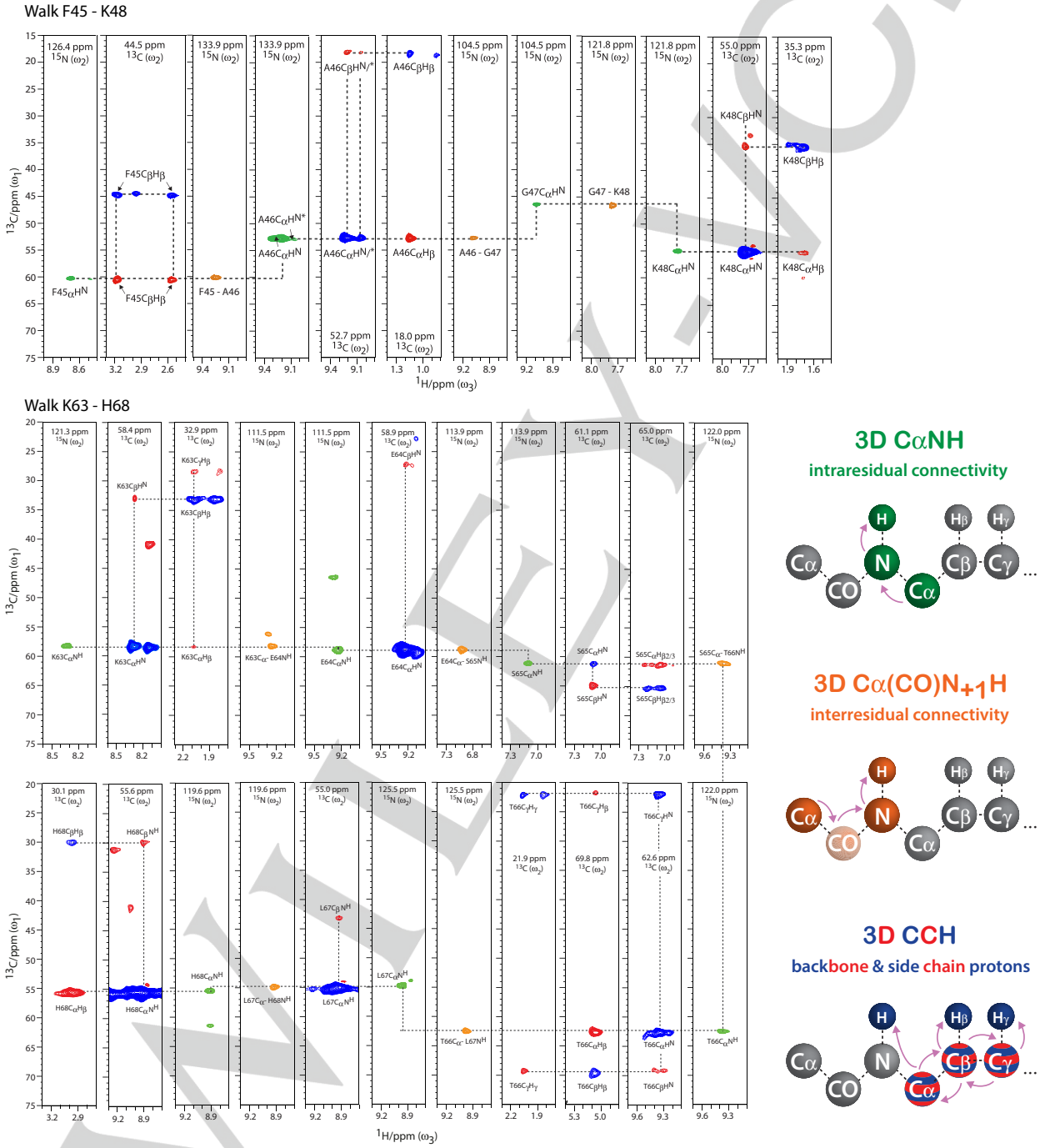

Figure S5. Backbone and side chain assignments in FD ubiquitin. Signals from 3D CαNH (green), 3D Cα(CO)NH (orange) and 3D CCH (blue for positive; red for negative signals) experiments, are color-coded. The transfer pathways in the 3D experiments are illustrated on the right. Double quantum DREAM[11] CC transfer was used in the 3D CCH experiment.

S3.2 FD KCSA

Sequential assignments in FD KcsA.

1. Using 3D CαNH and 3D CαCONH experiments, we could establish backbone walks (Figure S6). Note that our backbone assignment procedure benefited from the small number of H^N signals in FD KcsA. For more crowded spectra, further 3D experiments such as CONH and COCαNH would have been necessary. Moreover, by using a slightly longer ^{13}C to ^{1}H CP contact time, we obtained many sequential $C\alpha H^{N+1}$ contacts, which was a powerful and straightforward approach to validate our assignments (Figure S8B). In addition, we validated our backbone assignments with by 3D NHH experiment, in which we obtained many sequential H^N – H^N contacts (Figure S7).

2. Afterwards, we connected backbone and side chain information using i) a 2D C(C)H experiment (Figure S8B, in light blue) as well as ii) 2D and 3D NHH experiments (Figure 4C of the main text). These experiments allowed us to collect Cβ and Hβ information for a given residue, which together with our other data (H^N, N, Cα), gives a very good estimate to identify residue types. Moreover, in FD proteins the sheer presence or absence of correlations involving Hβ (see Table S1) provide further information on the residue type.

3. Finally, we also used 2D a CC RFDR[15] spectrum (Figure S9) as well as published chemical shift data to support our analysis.[16]

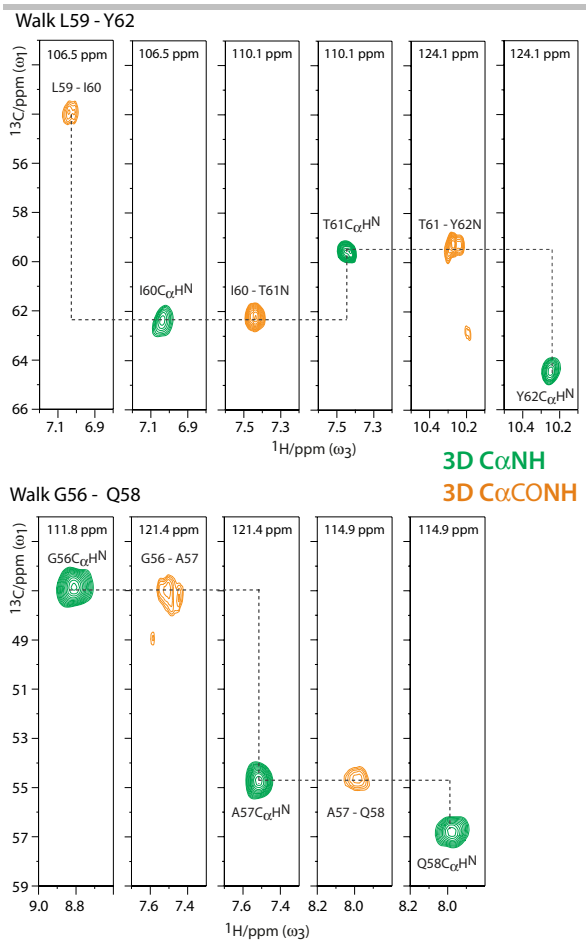

Figure S6. Examples for sequential backbone walks in FD KcsA (closed-conductive state). Strips were extracted from 3D CαNH (in green) and 3D CαCONH (orange) experiments.

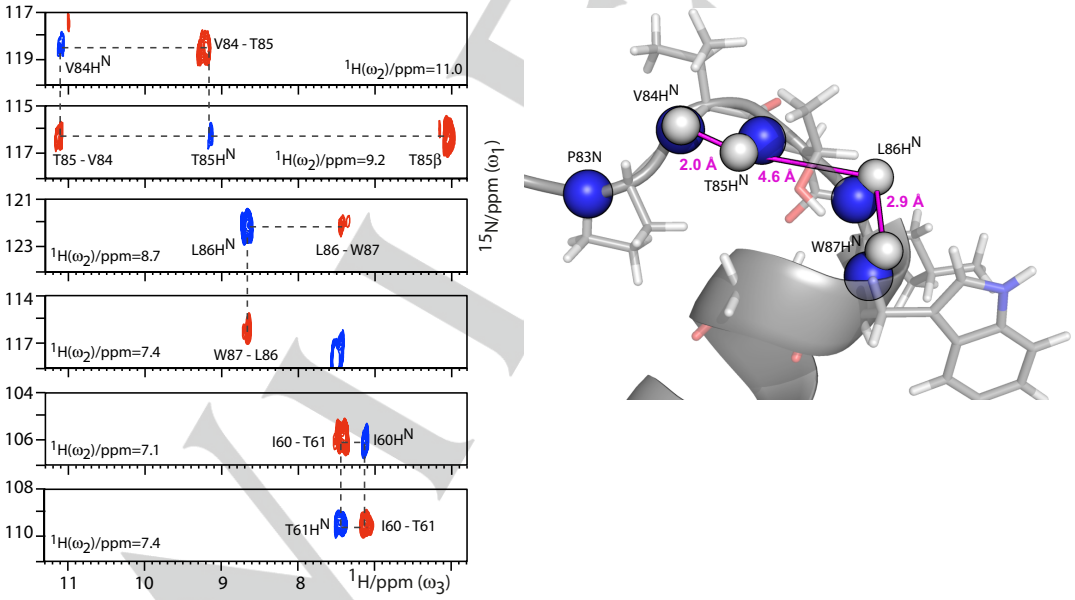

Figure S7. *Left*: Strips from a 3D NHH experiment using a short (750 us) DQ DREAM[11, 17] ^{1}H-^{1}H mixing block applied to closed-conductive FD KcsA. Positive and negative signals are shown in blue and red, respectively. This experiment allowed validating / assigning sequential H^N–H^N contacts. Moreover (see Figure 4C of the main text), it also readily allowed identifying residues based on i) the presence of intense Hβ signals and ii) the Hβ chemical shift. *Right*: Illustration of sequential contacts on Xray structure 1K4C. Note that the absence of a cross-peak between T85H^N – L86H^N is in very good agreement with the long (4.6 Å) distance between these protons in the Xray structure.

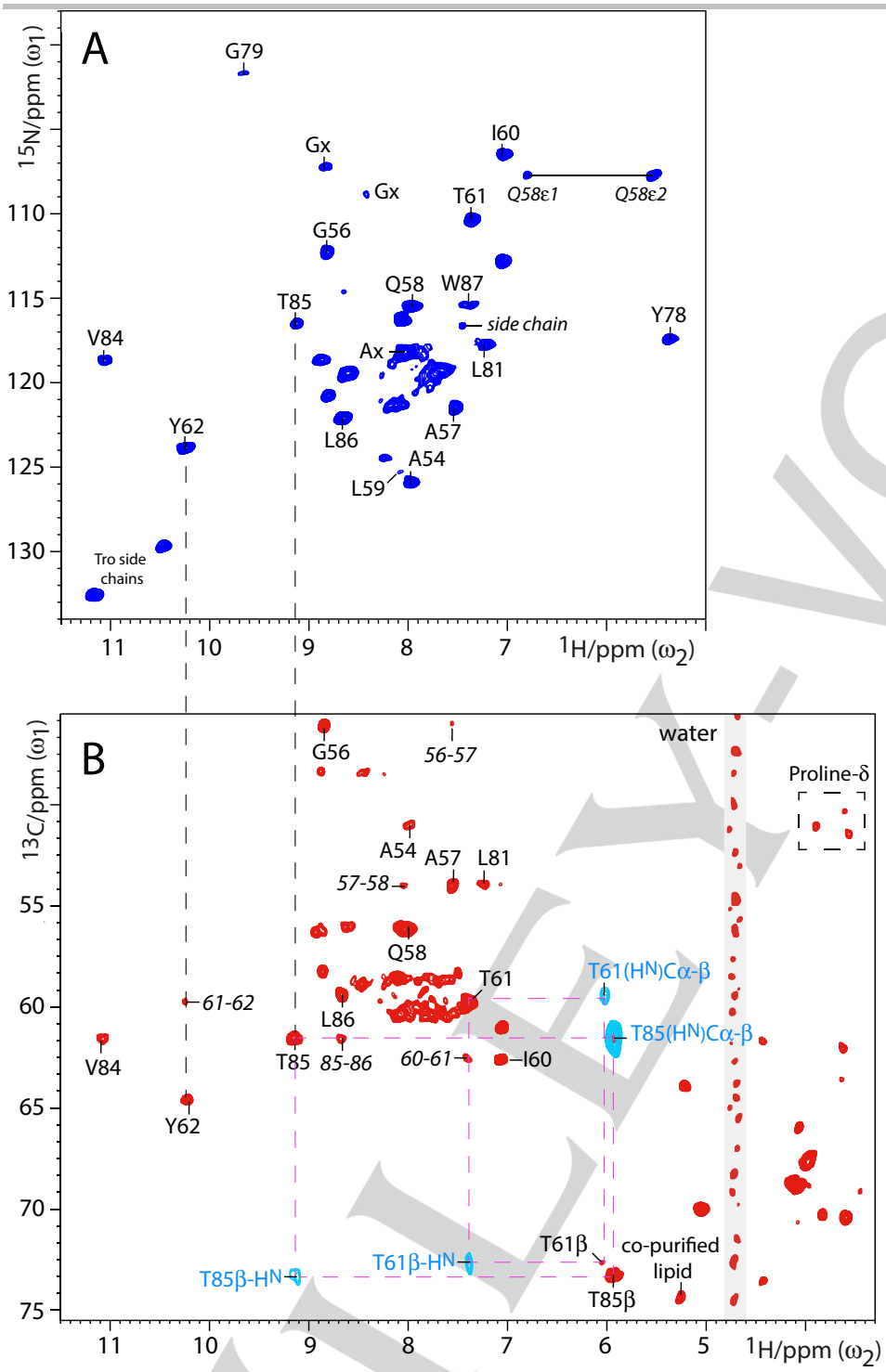

Figure S8. A) 2D NH spectrum of FD KcsA (closed-conductive). B) Cut-out of a 2D CH spectrum, which was measured with 700 µs CP contact time for the last ^{13}C to ^{1}H step. Next to intense CαH^{N} signals, we obtained many weaker CαH^{N+1} signals, which was a simple and very efficient way to cross-validate our sequential assignments. A cut-out of the negative intensity of a 2D C(C)H experiments using ^{13}C–^{13}C DREAM DQ mixing is superimposed (in light blue), in which Thr correlations Cβ-H^{N} and (H^{N})Cα-Hβ are visible. Such intra-residual correlations allowed identifying amino acids types based on Cβ and Hβ chemical shifts and based on the sheer presence or absence of correlations (see Table S1). Note signals detected on the side chain of T61 are much weaker than for T85, presumably due to enhanced dynamics, which is in line with the weak intensity of the transfer to Y62Hβ (Figure 4C of the main text), which agrees with the 2D N(H)H experiment, in which we did not observe transfer to T61Hβ. Noteworthy, T85Cβ (73.2 ^{13}C ppm) is the most low-field ^{13}C signal of KcsA, which implies that the signal at 74.4 13C ppm corresponds to a lipid-head group, mostly likely of ^{13}C labeled co-purified lipids.[18]

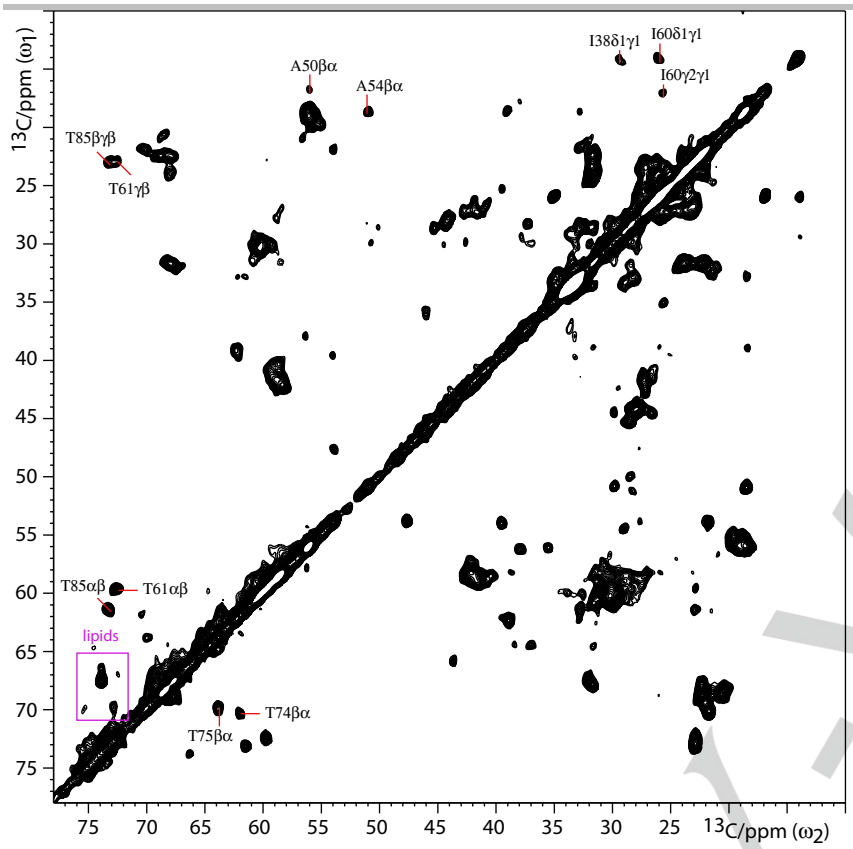

Figure S9. 2D ^{13}C-^{13}C RFDR[15] spectrum measured with closed-conductive FD KcsA. The spectrum was acquired with 3 ms CC mixing time.

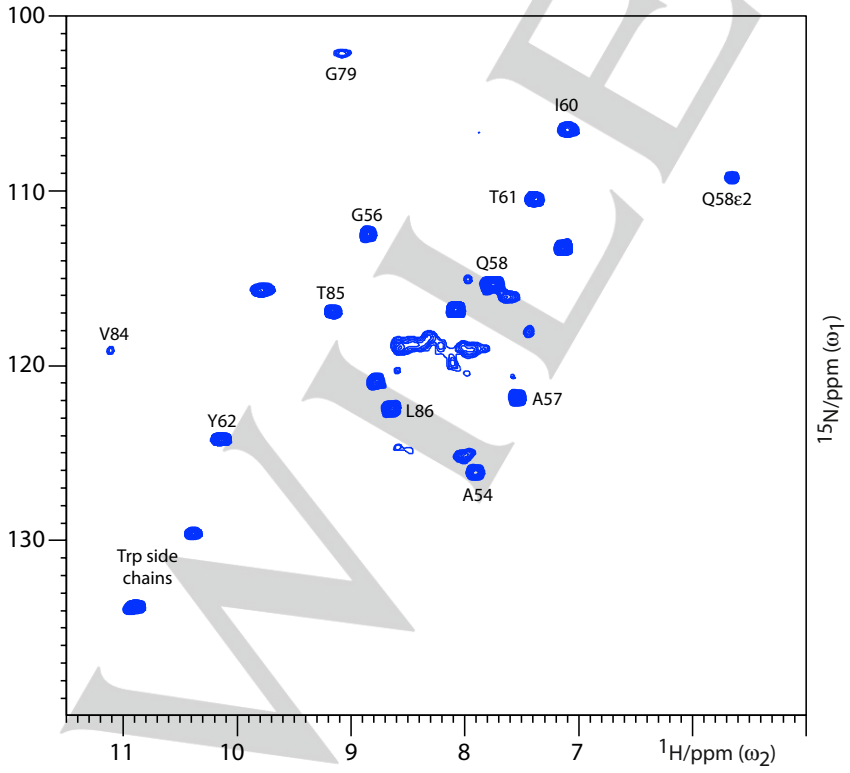

Figure S10. 2D NH spectrum of FD KcsA in the open-inactivated state carried out at 52 kHz MAS.

S4. FURTHER SUPPORTING FIGURES

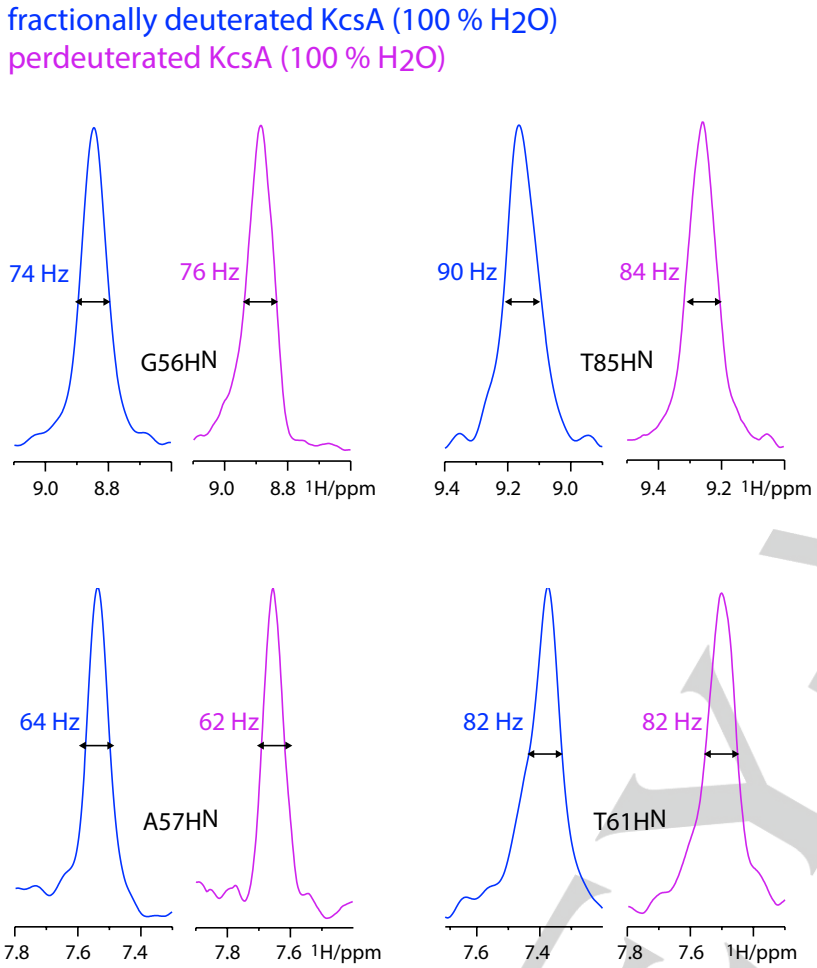

Figure S11. ^{1}H linewidth comparison between fractionally deuterated (FD, in blue) KcsA and perdeuterated (PD, in magenta) KcsA in the open-inactivated state. FD KcsA was measured at 52 kHz MAS and 800 MHz ^{1}H-frequency, PD KcsA was measured at 60 kHz MAS and 800 MHz ^{1}H-frequency. The spectrum used for the analysis of the ^{1}H linewidth in PD-KcsA can be found in Ref. ([19]). The comparison clearly shows that fractionally deuteration gives the virtually same H^{N} linewidth in KcsA as perdeuteration. This means that the availability of side chain ^{1}H in FD KcsA comes for free without resolution losses.

Moreover, while fractionally deuteration provides the same linewidth as perdeuteration, it avoids the use of expensive deuterated glucose and is hence much cheaper than perdeuteration.

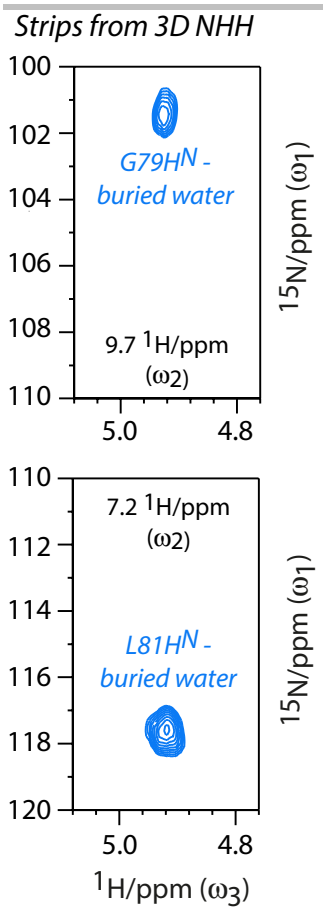

Figure S12. Strips extracted from a 3D NHH experiment with FD KcsA (closed-conductive), showing the two contacts to buried water that are discussed in the main text (Figure 3C,D). This experiment was necessary to confirm the contact L81H^N to buried water, given that several H^N signals resonant around 118 ^{15}N/ppm.

S5 SAMPLE PREPERATION

Fractionally deuterated ubiquitin was produced in a D_2O based M9 medium supplemented with 2 g/L ^{13}C-glucose and 0.5 g/L $^{15}NH_4Cl$. The fully protonated sample was produced in a H_2O based M9 medium supplemented with 2 g/L ^{13}C-glucose and 0.5 g/L $^{15}NH_4Cl$. Purification and further sample preparation steps were done as described in (Ref. [20]). The yield for the fractionally deuterated sample was 15 mg/l. *Fractionally deuterated KcsA* was expressed and purified as previously described,[16a] with the exception that D_2O instead of H_2O was used in the expression minimal medium. The yield for the FD channel was 11 mg/l. Reconstitution in *E. coli* polar lipids (Avanti) was performed at a 100/1 lipid/channel molar ratio using biobeads as previously described.[16a] After reconstitution, the fractionally deuterated channel was back-exchanged in fully protonated phosphate buffer (pH 7.0) and incubated for three weeks prior to the ssNMR measurements.

S6. REFERENCES

[1] G. Bodenhausen, D. J. Ruben, *Chem Phys Lett* **1980**, *69*, 185-189.

[2] G. Cornilescu, J. L. Marquardt, M. Ottiger, A. Bax, *Journal of the American Chemical Society* **1998**, *120*, 6836-6837.

[3] R. Otten, B. Chu, K. D. Krewulak, H. J. Vogel, F. A. Mulder, *Journal of the American Chemical Society* **2010**, *132*, 2952-2960.

[4] M. K. Rosen, K. H. Gardner, R. C. Willis, W. E. Parris, T. Pawson, L. E. Kay, *Journal of molecular biology* **1996**, *263*, 627-636.

[5] aV. Agarwal, S. Penzel, K. Szekely, R. Cadalbert, E. Testori, A. Oss, J. Past, A. Samoson, M. Ernst, A. Bockmann, B. H. Meier, *Angewandte Chemie* **2014**, *53*, 12253-12256; bJ. M. Lamley, D. Iuga, C. Oster, H. J. Sass, M. Rogowski, A. Oss, J. Past, A. Reinhold, S. Grzesiek, A. Samoson, J. R. Lewandowski, *Journal of the American Chemical Society* **2014**, *136*, 16800-16806.

[6] D. H. Zhou, C. M. Rienstra, *Journal of magnetic resonance* **2008**, *192*, 167-172.

[7] M. Weingarth, G. Bodenhausen, P. Tekely, *J Magn Reson* **2009**, *199*, 238-241.

[8] T. Sinnige, M. Daniels, M. Baldus, M. Weingarth, *Journal of the American Chemical Society* **2014**, *136*, 4452-4455.

[9] E. K. Paulson, C. R. Morcombe, V. Gaponenko, B. Dancheck, R. A. Byrd, K. W. Zilm, *Journal of the American Chemical Society* **2003**, *125*, 15831-15836.

[10] M. Baldus, A. T. Petkova, J. Herzfeld, R. G. Griffin, *Mol Phys* **1998**, *95*, 1197-1207.

[11] R. Verel, M. Baldus, M. Ernst, B. H. Meier, *Chem Phys Lett* **1998**, *287*, 421-428.

[12] D. J. Holland, M. J. Bostock, L. F. Gladden, D. Nietlispach, *Angew Chem Int Edit* **2011**, *50*, 6548-6551.

[13] M. Veshtort, R. G. Griffin, *Journal of magnetic resonance* **2006**, *178*, 248-282.

[14] M. J. Bayro, M. Huber, R. Ramachandran, T. C. Davenport, B. H. Meier, M. Ernst, R. G. Griffin, *The Journal of chemical physics* **2009**, *130*, 114506.

[15] A. E. Bennett, J. H. Ok, R. G. Griffin, S. Vega, *The Journal of chemical physics* **1992**, *96*, 8624-8627.

[16] aE. A. van der Cruijsen, D. Nand, M. Weingarth, A. Prokofyev, S. Hornig, A. A. Cukkemane, A. M. Bonvin, S. Becker, R. E. Hulse, E. Perozo, O. Pongs, M. Baldus, *Proceedings of the National Academy of Sciences of the United States of America* **2013**, *110*, 13008-13013; bR. Schneider, C. Ader, A. Lange, K. Giller, S. Hornig, O. Pongs, S. Becker, M. Baldus, *Journal of the American Chemical Society* **2008**, *130*, 7427-7435; cJ. H. Chill, J. M. Louis, J. L. Baber, A. Bax, *Journal of biomolecular NMR* **2006**, *36*, 123-136; dB. J. Wylie, M. P. Bhate, A. E. McDermott, *Proceedings of the National Academy of Sciences of the United States of America* **2014**, *111*, 185-190.

[17] M. Huber, S. Hiller, P. Schanda, M. Ernst, A. Bockmann, R. Verel, B. H. Meier, *Chemphyschem : a European journal of chemical physics and physical chemistry* **2011**, *12*, 915-918.

[18] M. Weingarth, A. Prokofyev, E. A. W. van der Cruijsen, D. Nand, A. M. J. J. Bonvin, O. Pongs, M. Baldus, *Journal of the American Chemical Society* **2013**, *135*, 3983-3988.

[19] M. Weingarth, E. A. van der Cruijsen, J. Ostmeyer, S. Lievestro, B. Roux, M. Baldus, *Journal of the American Chemical Society* **2014**, *136*, 2000-2007.

[20] T. Sinnige, M. Daniels, M. Baldus, M. Weingarth, *Journal of the American Chemical Society* **2014**, *136*, 4452-4455.